NOVEL B/ZnO MATERIAL FOR ENHANCED DEGRADATION OF TETRACYCLINE HYDROCHLORIDE IN AN AQUEOUS ENVIRONMENT UNDER VISIBLE LIGHT

VẬT LIỆU B/ZnO MỚI GIÚP TĂNG CƯỜNG PHÂN HỦY TETRACYCLINE HYDROCHLORIDE TRONG MÔI TRƯỜNG NƯỚC DƯỚI ÁNH SÁNG KHẢ KIẾN

Nguyen Thu Huong[1], Vu Anh Tuan[1], Nguyen Minh Viet[2,*]

DOI: http://doi.org/10.57001/huih5804.2024.096

ABSTRACT

In this study, the B/ZnO materials were simply synthesized via a Sol-gel method. The photocatalytic ability of materials was evaluated by degrading tetracycline hydrochloride (TCH). The characteristics of the ZnO and 3B/ZnO materials were analyzed and evaluated by the Diffuse Reflectance Ultraviolet-Visible (DR/UV-Vis), Scanning Electron Microscope (SEM), Fourier Transform Infrared Spectroscopy (FT-IR), and X-Ray Diffraction (XRD) techniques. The 3B/ZnO material had a band gap energy of 3.15eV. It was relatively rough and the nanoparticles were more compact and had a higher photocatalytic efficiency than ZnO with the TCH degradation efficiency achieved at 92.28%, and a rate constant of 0.048min^{-1}. Thus, the optimal doped B was 3 wt%. The factors that affect the photocatalytic process such as the initial TCH concentration, the catalyst content, and the pH solution were comprehensively investigated.

Keywords: *B/ZnO, antibiotic, tetracycline hydrochloride, photocatalysis.*

TÓM TẮT

Trong nghiên cứu này, các vật liệu B/ZnO được tổng hợp đơn giản bằng phương pháp Sol-gel. Khả năng quang xúc tác của các vật liệu được đánh giá bằng khả năng phân hủy tetracycline hydrochloride (TCH). Các đặc tính của vật liệu ZnO và 3B/ZnO được phân tích và đánh giá bằng máy đo tia cực tím phản xạ khuếch tán (DR/UV-Vis), kính hiển vi điện tử quét (SEM), quang phổ hồng ngoại biến đổi Fourier (FT-IR) và kỹ thuật nhiễu xạ tia X (XRD). Vật liệu 3B/ZnO có năng lượng vùng cấm là 3,15eV. Nó tương đối thô và các hạt nano nhỏ gọn hơn và có hiệu suất xúc tác quang cao hơn ZnO với hiệu suất phân hủy TCH đạt được ở mức 92,28% và hằng số tốc độ là 0,048 phút^{-1}. Do đó, lượng pha tạp B tối ưu là 3% trọng lượng. Các yếu tố ảnh hưởng đến quá trình quang xúc tác như nồng độ TCH ban đầu, hàm lượng chất xúc tác, pH của dung dịch đều được nghiên cứu một cách toàn diện.

Từ khóa: *B/ZnO, kháng sinh, tetracycline hydrochloride, xúc tác quang.*

[1]School of Chemistry and Life Sciences, Hanoi University of Science and Technology, Vietnam

[2]Faculty of Chamical Technology, Hanoi University of Industry, Vietnam

[*]Email: minhviet@haui.edu.vn

Ngày nhận bài: 06/01/2024

Ngày nhận bài sửa sau phản biện: 05/3/2024

Ngày chấp nhận đăng: 25/3/2024

1. INTRODUCTION

Every year, large amounts of antibiotics are administered to both humans and animals to treat diseases and infections [1-3]. In animal husbandry, antibiotics are often administered to livestock at sub-therapeutic levels to prevent disease and promote growth [4-6]. Especially, antibiotics are used to prevent, treat diseases, and promote growth in aquaculture [7-10]. There are many kinds of antibiotics used in aquaculture including aminoglycosides, quinolones, sulfonamides, tetracyclines, macrolides, β-lactams, nitrofurans, and lincosamides, etc [11]. In many nations, antibiotic usage in aquaculture is largely unregulated. For example, antibiotics have been the most used in Vietnam, followed by Chile, and Korea. In aquaculture, antibiotics are used by mixing the antibiotic substances with feed, pond sprinkling, and injection. All the above methods, aside from injection, have a direct impact on the aquatic environment. Many studies show that fish did not effectively metabolized antibiotics and about 75% of the antibiotics fed to fish are excreted back into the aquatic environment [12]. The presence of antibiotics in the aquatic environment is a major concern because these pollutants have potential adverse effects on ecosystems, increase the development of antibiotic-resistant pathogens, and can pose threats to human health [1, 13, 14]. Antibiotic contamination in water also poses many challenges to the water treatment industry.

Currently, there are many methods to treat antibiotic contaminants in water such as physical adsorption, biodegradation, advanced oxidation, coagulation, and electrolysis, etc [2, 15, 16]. In which, photocatalysis is a promising method in the field of water treatment in general as well as the treatment of antibiotic pollution. Photocatalysis is a method that uses light as an energy source to activate a catalyst that speeds up a chemical reaction without being consumed in the reaction [17-20]. Photocatalysis has several advantages, including the ability

to occur at room temperature as well as the ability to almost decompose organic pollutants completely into CO_2, H_2O, and N_2, especially this method takes advantage of solar light sources leading to saving costs in the processing process. This is considered a green, environmentally friendly chemical method, which has been widely researched and developed at home and abroad.

Some semiconductor materials have been widely studied, including zinc oxide (ZnO), titanium oxide (TiO_2), and g-C_3N_4, etc [21-23]. In which, zinc oxide (ZnO) has attracted the attention of many researchers because of its ease of synthesis, low cost, non-toxicity, and large band gap energy (3.37eV) [24]. Under the radiation of light, the electrons and holes created by ZnO can decompose organic substances. However, there are also some limitations when using ZnO as a photocatalyst, such as low sunlight absorption due to high band gap energy, and the electron-hole recombination process taking place rapidly emerging has limited its practical applications. To improve the photocatalytic performance of ZnO, people often doped an appropriate number of metals such as gold (Au), silver (Ag), tin (Sn)... or nonmetals such as boron (B), and nitrogen (N),... [25-27] both enhance the ability to absorb sunlight, and at the same time prevent the recombination between electrons and holes, improve the particle size, increase the surface area, and bring about the photocatalytic ability effective decomposition of organic matter. Among them, B doping has attracted great interest due to its atomic size and electronic structure [13, 28]. Currently, there are many different methods for doping B on ZnO such as the sol-gel method, and combustion method.

In this study, the B/ZnO material was synthesized by the sol-gel method. Material properties are analyzed through various measurements including the scanning electron microscopy (SEM), the X-ray powder diffraction (XRD), the Fourier transform infrared spectroscopy (FT-IR), and the diffuse reflectance Ultraviolet-Visible spectra (DR/UV-Vis). The photocatalytic ability of the material was evaluated by the degradation efficiency of tetracycline hydrochloride (TCH) in water. The effect of doped B content on photocatalytic efficiency was also studied. The factors affecting the photocatalysis process were also studied, including the catalyst content, the initial TCH concentration, and the pH solution. The mechanism of TCH degradation was also investigated.

2. MATERIALS AND METHODS

2.1. Material

All chemicals used in the synthesis of the material were purchased from Germany including zinc acetate dehydrates ($Zn(CH_3COO)_2.2H_2O$, 99%), boric acid (H_3BO_3, 99.8%), sodium hydroxide, and ethanol. Tetracycline hydrochloride ($C_{22}H_{24}N_2O_8.HCl$, 99%) was purchased from Hefei BoMei Biotechnology Co., Ltd, China. All chemicals are used directly, and distilled water is used during the evaluation of the photocatalytic potential of the material.

2.2. Methods

The light absorption and band gap energy of the composites were determined by the diffuse reflectance Ultraviolet-Visible spectra (DR/UV-Vis). An X-ray diffraction (German) was used to analysis the characteristic of the synthesized materials. It was equipped with Cu Kα radiation (λ = 1.54060Å) at 25°C. The 2θ range was scanned from 5 to 80°, and the generator was set at 35mA and 40kV. The surface morphology of the synthesized materials was observed by A scanning electron microscope (SEM JEOL serios 7600F), and the landing voltage was 10.0kV. The identification of functional groups presents, and intermolecular bonding characteristics of the synthesized materials were analyzed by a Fourier transform infrared spectrometer (FT-IR, Thermos Scientific - NICOLET iS50FT-IR). The wavenumber was studied from 4000 to 400cm^{-1}.

2.3. Preparation of the materials

The material preparation procedure is presented in Figure 1. Typically, 4.4444g of zinc acetate dehydrates and x g of boric acid were dissolved in 50 mL of ethanol and stirred at room temperature (25°C) for 1h. After, the 2.0N NaOH solution was added to this mixture to adjust the pH solution (pH = 8). This mixture was stirred at 60°C for 3 h to obtain a white gel which was sealed with cling film and incubated overnight. Then, this gel was filtered and washed with distilled water and ethanol to remove the impurities and residual substances. The white precipitate was dried for 24 h at 80°C and ground into the fine powders. Finally, this precipitate was calcined at 500°C for 4h to obtain the B/ZnO composites. Samples are stored in sealed flasks before being used for analysis and catalysis. The boron content was investigated at 1, 3, 5, and 7 wt%, and the synthesized materials were named 1B/ZnO, 3B/ZnO, 5B/ZnO, and 7B/ZnO, respectively. The ZnO sample was produced using the same procedure with composite but without boric acid.

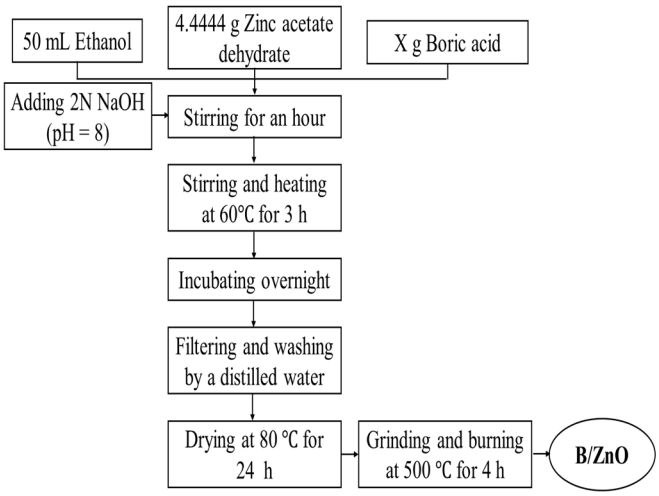

Figure 1. The B/ZnO material synthesis process

2.4. Photocatalysis ability evaluation process

The photocatalytic ability of the materials was evaluated by the degradation efficiency of tetracycline hydrochloride

(TCH) in water. A UV-Vis spectrophotometer (Agilent 8453) was used to determine the TCH concentration. The experimental procedure is conducted as follows: a g catalyst was added to a beaker containing 100mL TCH b mg/L and sonicated for about 5 min to disperse the material evenly. This mixture was stirred at 250rpm continuously in the dark to get an adsorption/desorption equilibrium for 30 min. Then this mixture was irradiated with a 250W Hg lamp. After given time intervals, 3mL suspension was filtered through a filter, and measured residual TCH concentration. The equation (1) and (2) were used to evaluate the degradation efficiency (DE) and rate constant of TCH, respectively [14]:

$$DE(\%) = \frac{C_0 + C}{C_0} x100 \quad (1)$$

$$\ln\frac{C_0}{C} = kt \quad (2)$$

Where: C is the solution concentration at time t; C_o is the initial solution concentration; k is the rate constant; t is the time.

3. RESULTS AND DISCUSSION

3.1. The optimal B content

A material's ability to absorb light is one of the factors that determine its photocatalytic ability. The DR/UV-Vis method was used to evaluate the adsorption light ability of the synthesized materials and the results are shown in Figure 2(a). All synthesized materials strongly absorb light in the region 250 - 356nm and significantly reduce adsorption above 400nm. The steep adsorption slope is 360 - 400nm. The 7B/ZnO material had weaker adsorption compared to all synthesized materials. The band gap energy of the synthesized materials was calculated by the Tauc's equation and the results are shown in Figure 2(b). The band gap energy of the 7B/ZnO material is 3.17eV, the other materials had the similar band gap energy value of 3.15eV.

The photocatalytic ability of the synthesized materials was evaluated through the TCH degradation efficiency in a water environment with the following reaction conditions: [TCH] = 20mg/L, [catalyst] = 0.5g/L, and a 250W Hg lamp. The results are shown in Figure 2(c). The photocatalysis ability of the ZnO and 1B/ZnO materials was similar with the DE value of 68.45%. When the B content increases to 3 wt%, the DE value and rate constant also increase (DE = 92.28% and k = 0.048min^{-1}). When B content increases, the TCH degradation efficiency tends to increase. However, when the B content increase to 5 and 7 wt%, the DE value and rate constant decrease. The DE value was 82.58% and the rate constant was 0.015min^{-1} for the 7B/ZnO material. For the 5B/ZnO material, the DE value and rate constant were 81.55% and 0.016min^{-1}, respectively. Thus, the 3B/ZnO material has the best photocatalytic ability. This result is consistent with the results of light absorption and band gap energy research of the material studied above. And this material was chosen for further study.

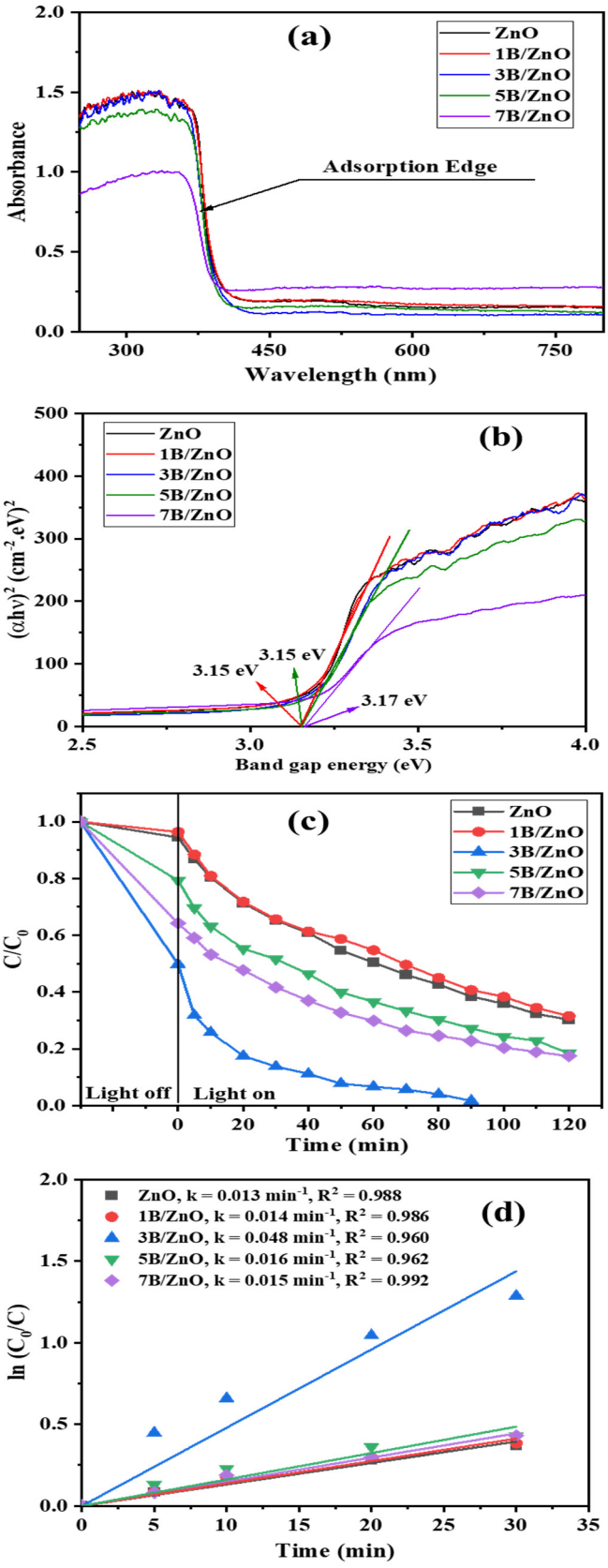

Figure 2. (a) The DR/UV-Vis spectra and (b) the Tauc plots, (c) the TCH degradation efficiency of the materials, and (d) kinematic curves. Conditions: [TCH] = 20mg/L, [catalyst] = 0.5g/L, and a 250W Hg lamp.

3.2. Compare the characteristics of the ZnO and 3B/ZnO materials

The SEM analysis results of the ZnO and 3B/ZnO materials are shown in Figure 3(a-b). The morphology of the ZnO material was clear and consisted of nanoparticles with a size of about 42 - 79nm that conglomerated and tightly arranged together. The appearance of B significantly changed the size and aggregation state of the nanoparticles. The size of the nanoparticles was smaller (about 15nm) than the nanoparticles of the ZnO material. The morphology of the 3B/ZnO material was relatively rough and the nanoparticles were more compact. This may be one of the reasons for the enhanced photocatalytic degradation of 3B/ZnO material.

The XRD analysis results (Figure 3(c)) show that doping additional B onto the ZnO material does not change the original structure of the material. Both materials give peaks at planes characteristic of the hexagonal wurtzite structure of ZnO (JCPDS 36-1451) [19]. The intensity of the peaks of the 3B/ZnO material was lower than the ZnO material. Moreover, the peaks of boron were not appeared. This can be explained by the low content and low crystallinity of B in the 3B/ZnO material. The crystal size of the ZnO and 3B/ZnO material was calculated by the Scherrer equation. The crystallite size of ZnO and B/ZnO materials was 17.68, and 12.11nm, respectively. Calculation results show that the appearance of boron in the 3B/ZnO material causes the crystal size of this material to decrease significantly. This may be the reason for the enhanced photocatalytic degradation of TCH of the 3B/ZnO material.

The FT-IR analysis results of the ZnO and 3B/ZnO material (Figure 3(d)) show the function groups in the materials. The peaks between 698 and 924cm^{-1} of the ZnO and B/ZnO materials characterize the vibrations of the O-H bond in ZnO-O-H [17]. The peaks at 3417 and 3450cm^{-1} characterize the stretching vibration of the intermolecular hydrogen bond (O-H) of water molecules adsorb on the surface of the ZnO and 3B/ZnO materials [29]. Especially, on the spectrum of the 3B/ZnO material, the peak appears at 1252cm^{-1}, which characterizes the valence vibration of the B-O bond [13, 14, 28]. This can prove that the B has been successfully doped onto the ZnO material.

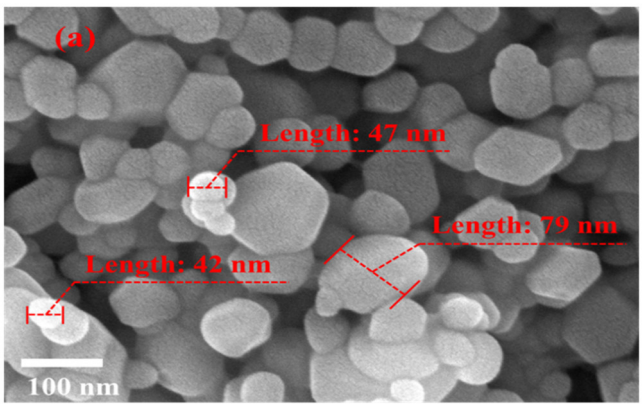

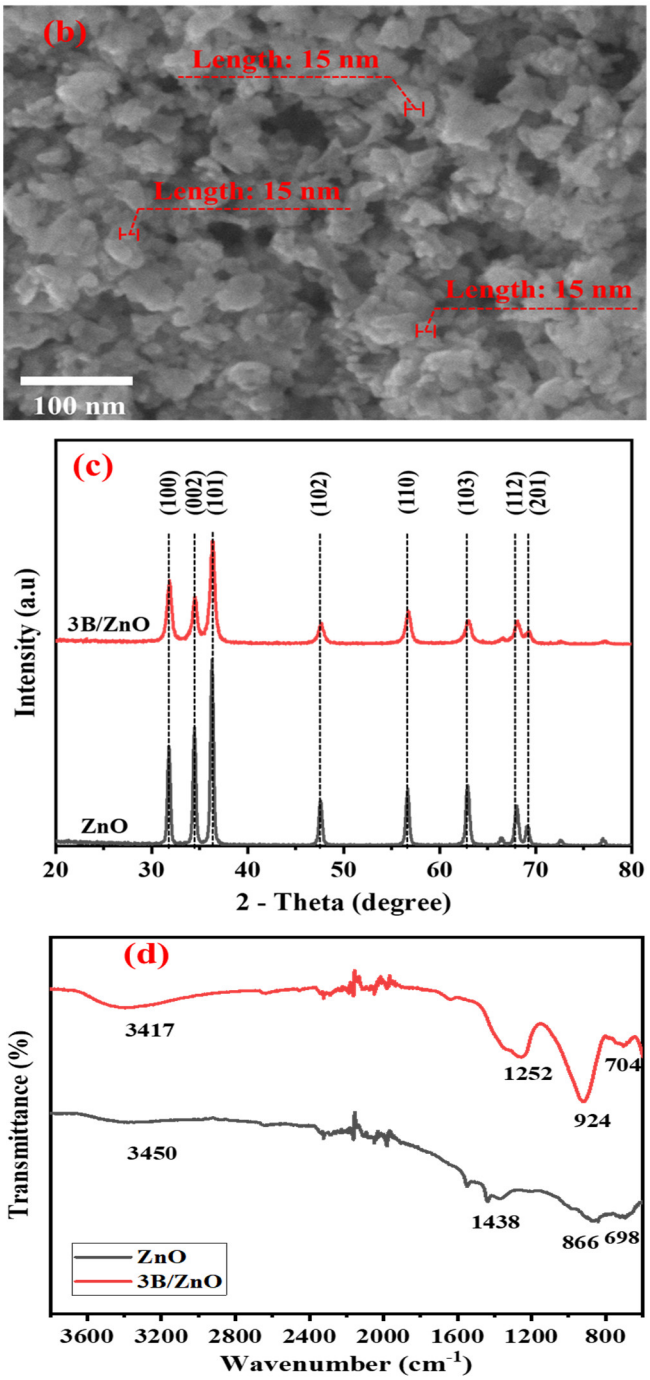

Figure 3. The SEM image of the (a) ZnO and (b) 3B/ZnO material, (c) the XRD and (d) FT-IR spectra of the materials

From the results of the analysis and comparison of the characteristics of ZnO and 3B/ZnO materials, we can draw the following conclusions: The presence of B does not change the structure of the ZnO material. The size of the 3B/ZnO material was smaller than the ZnO material. The nanoparticles of the 3B/ZnO material were smaller and more compact than those of the ZnO material. The morphology of the 3B/ZnO material becomes rougher. These are also the reasons why the 3B/ZnO material has a better photocatalytic ability to degrade TCH than the ZnO material.

3.3. The factors affecting the photocatalytic process of the 3B/ZnO material

3.3.1. Effect of the pH of the TCH initial solution

The pH value is one of the criteria for evaluating water quality and is also a factor affecting the wastewater treatment process. In this study, the pH values were evaluated about the range of 2 - 11. The other experimental conditions are fixed as follows: [TCH] = 20mg/L, [3B/ZnO] = 0.5g/L, room temperature (25°C), and a 250W Hg lamp. The research results are presented in Figure 4. Figure 4(a) shows the correlation between changing the pH value and changing the light absorption area of the antibiotic TCH. The pH value also affects the existence of TCH in solution because TCH has 3 pK_a and this can affect the photocatalytic process [13]. The pH_{pzc} value of the 3B/ZnO material was determined to be 7.6 (Figure 4(b)). When the pH value of the initial TCH solution is less than the pH_{pzc} value, the surface of the 3B/ZnO material is positively charged and vice versa. The photocatalytic efficiency of TCH degradation at the different pH conditions is presented in Figure 4(c-d). At pH = 2, the photocatalytic degradation of TCH is very slow (k = 0.001min^{-1}), and the DE is very low (DE = 8.58%). At too low a pH value, the 3B/ZnO material may partially dissolve; both the 3B/ZnO and TCH materials are positively charged, leading to very poor interaction between the material and TCH molecules. These make it difficult for the photocatalytic process to occur. At pH = 6, the TCH molecules do not dissociate and the 3B/ZnO material surface is positively charged, leading to better interaction between the TCH molecules and 3B/ZnO material. This can be proven by the TCH adsorption efficiency (52.49%) and is also a good condition for the photocatalytic degradation of TCH to proceed more smoothly (DE = 94.05% and k = 0.042min^{-1}). At pH = 9, the TCH molecules dissociate into cations and the 3B/ZnO material surface is negatively charged, leading to the interaction between the TCH molecules and 3B/ZnO material is the best. The TCH adsorption efficiency of 62.33% is the highest. At this pH, the photocatalytic decomposition of TCH also takes place smoothly with the DE value of 95.49 %, and the rate constant of 0.042min^{-1}. At pH = 11, the TCH molecules dissociate into anions and the 3B/ZnO material surface is negatively charged, leading to the interaction between the TCH molecules and 3B/ZnO material is the worst. The TCH adsorption efficiency was only 21.65%. However, the DE value and rate constant still achieved 94.99% and 0.045min^{-1}, respectively. This can be explained that at pH = 11, creating the presence of a large amount of OH^- ions on the 3B/ZnO material surface as well as in the reaction environment, creating conditions for the formation of •OH. As a result, the reaction rate increases slightly and the DE value almost unchanged. Thus, the pH value of the initial TCH solution greatly affects the photocatalytic decomposition of TCH in a water environment. For convenience in wastewater treatment, the pH value chosen is the most optimal condition of 6.

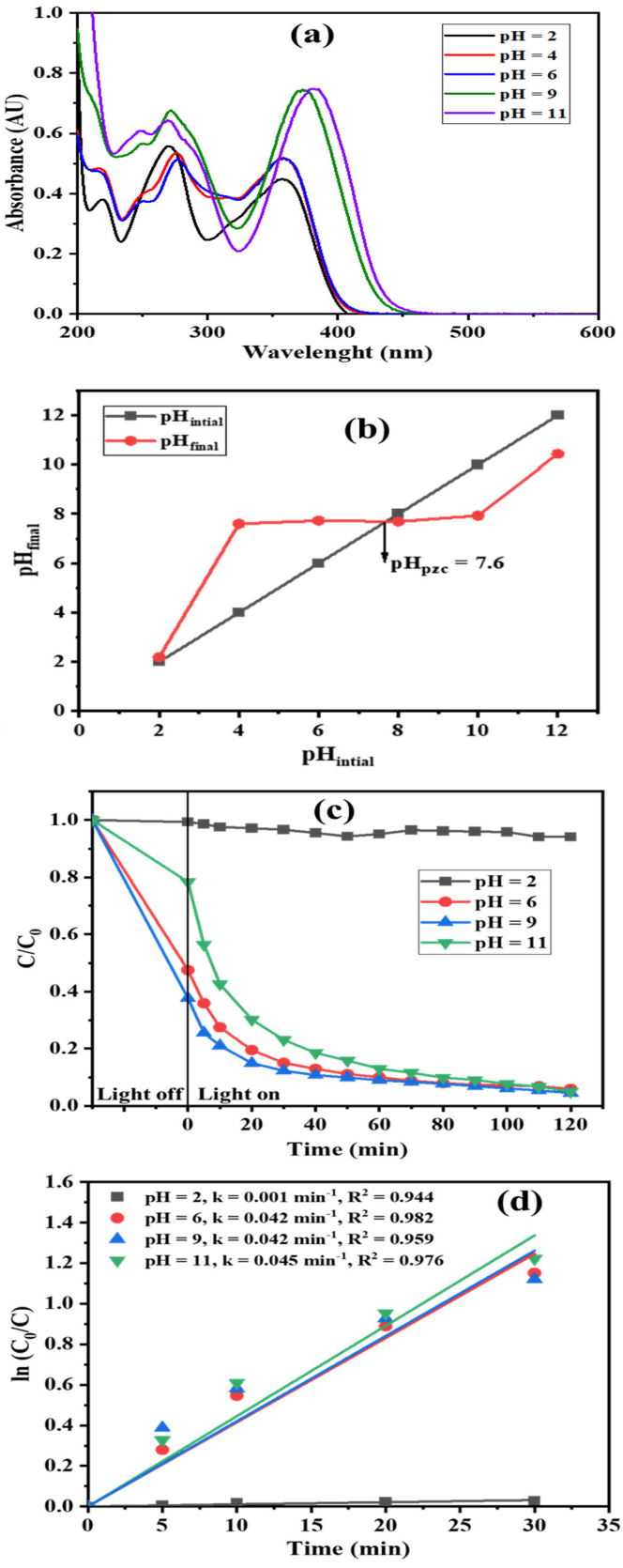

Figure 4. (a) The UV-Vis spectra of the TCH at different pH values, (b) the pH_{pzc} value of the 3B/ZnO material, (c) the TCH degradation efficiency of the 3B/ZnO material at different pH values, and (d) kinematic curves. Conditions: [TCH] = 20mg/L, [3B/ZnO] = 0.5g/L, and a 250W Hg lamp

3.3.2. Effect of the 3B/ZnO material content

Figure 5 shows the effect of the 3B/ZnO material content on the degradation of TCH. When the 3B/ZnO content used increased from 0.25g/L to 1.00g/L, the DE value also increased under the same reaction conditions of the initial TCH concentration of 20 mg/L and the light source is a 250W Hg lamp. As Figure 5(a), it can see that in 120 min, using the 3B/ZnO material content of 0.25g/L had the DE value of 73.98%, with the 3B/ZnO material content of 1.00g/L had the DE value of 95.36%. The rate constant values corresponding to the 0.25, 0.50, 0.75, and 1.00g/L of the 3B/ZnO material content are 0.015, 0.026, 0.037, and 0.046min^{-1}, respectively. The effect of the 3B/ZnO material content on the photocatalytic degradation TCH process can be explained by the following reasons: the 3B/ZnO material content increases leading to the number of active sites available on the catalyst surface and increasing the density of catalyst particles in the illuminated area. Therefore, the photocatalytic degradation of TCH proceeds more smoothly leading to a rapid increase in the TCH photodegradation efficiency. As a result, the DE value and reaction rate can be improved when increasing the 3B/ZnO material content. The optimal 3B/ZnO material content was chosen as 0.5g/L.

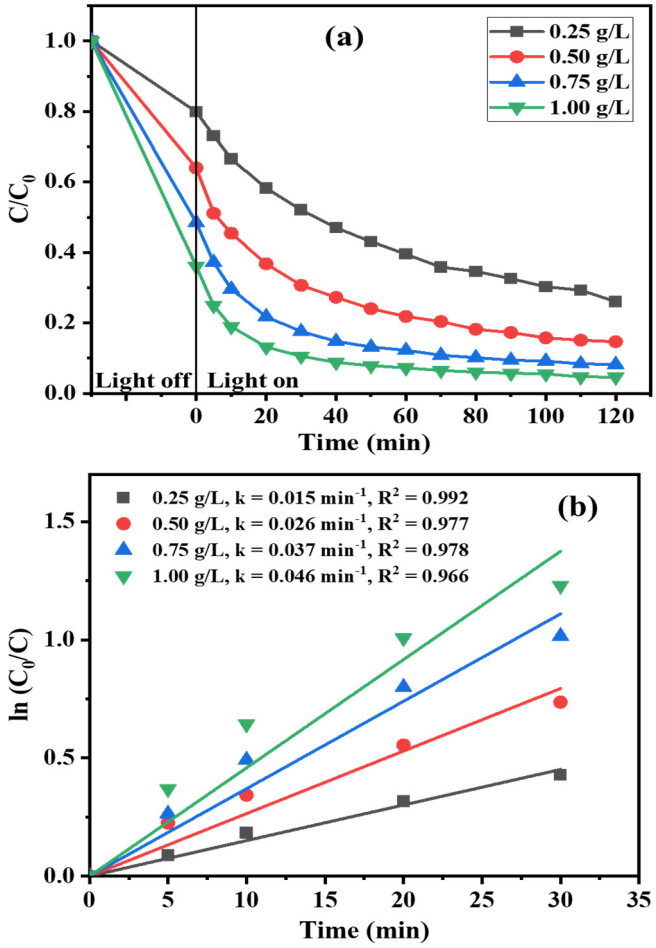

Figure 5. (a) The TCH degradation efficiency with the different 3B/ZnO material contents, and (d) kinematic curves. Conditions: [TCH] = 20mg/L, [3B/ZnO] = 0.25 - 1.00g/L, and a 250W Hg lamp

3.3.3. Effect of the initial TCH concentration

The initial TCH solution concentration was investigated in the range of 15 - 30mg/L under the same reaction conditions with the 3B/ZnO material content of 0.5g/L, and a 250W Hg lamp and the results are shown in Figure 6. It can be seen that an increase in the initial TCH concentration causes a decrease in the degradation efficiency, which reflects the law. With the initial TCH concentration of 15mg/L, it will be completely decomposed in about 60 minutes. Meanwhile, it takes 120 minutes to degrade 82.73% of TCH with the initial TCH concentration of 30 mg/L. The rate constants with initial concentrations of 15, 20, 25, and 30mg/L in the presence of the 3B/ZnO material are 0.061, 0.048, 0.034, and 0.026min^{-1}, respectively. This result can be explained by the following reasons: When increasing the initial TCH concentration, photons are blocked before they can reach the catalyst surface, and the generation of $\bullet OH^-$ and $\bullet O^{2-}$ radicals decreases, leading to the efficiency and rate of TCH degradation decreases. Additionally, a large amount of adsorbed antibiotics can compete for the constant total number of active sites available for adsorption at the fixed 3B/ZnO material content. The optimal initial TCH concentration was chosen as 20mg/L.

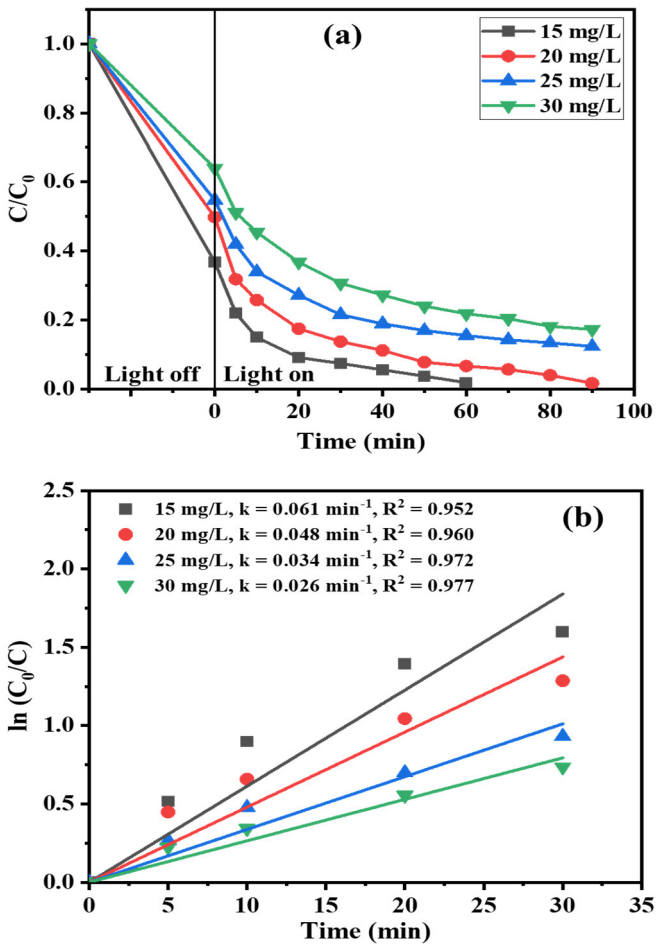

Figure 6. (a) The TCH degradation efficiency of the 3B/ZnO material with the different TCH concentrations, and (d) kinematic curves. Conditions: [TCH] = 15 - 30mg/L, [3B/ZnO] = 0.5g/L, and a 250W Hg lamp

3.4. Photocatalytic mechanism of the 3B/ZnO material

The photocatalytic mechanism of TCH decomposition of 3B/ZnO material is described in Figure 7. When irradiated by a light source with energy equal to or greater than the band gap energy of 3B/ZnO material (3.15eV), electrons (e^-) in the valence band (VB) will be excited and move to the conduction band (CB) with a higher energy level, while leaving a hole (h^+) in VB. Electron-hole pairs (e^- and h^+) move to the surface of the 3B/ZnO material to perform oxidation-reduction reactions that generate radicals including superoxide anion ($•O^{2-}$) and hydroxyl radical (•OH). Therefore, in the CB region of the 3B/ZnO material, the electrons easily react with O2 to create $•O^{2-}$, then $•O^{2-}$ radicals continue to interact with H_2O adsorbed on the surface of the material to create hydrogen peroxide (H_2O_2). H_2O_2 can react with electrons or $•O^{2-}$ radicals, or even photo light leading to the formation of •OH radicals. On the other hand, in the VB region of the 3B/ZnO material, the H2O molecules are oxidized by the holes to form •OH radicals. Reactive oxygen species such as •OH, $•O^{2-}$ and H_2O_2 are strong oxidizing agents that will attack TCH molecules adsorbed on the surface of 3B/ZnO material to quickly form intermediate compounds. Through the processes of hydrogenation, oxidation, and mineralization, intermediate compounds will eventually be converted into harmless compounds such as CO_2 and H_2O.

With the electron deficiency characteristic of B, the B is considered an electron trap in the 3B/ZnO material. Therefore, it will attract electrons toward it leading to a decrease decreased the electron and hole recombination time. In addition, it also attracts OH- toward the surface of the 3B/ZnO material leading to the process of creating OH radicals also taking place more smoothly. Therefore, the 3B/ZnO material has better TCH photocatalytic degradation ability than the ZnO material.

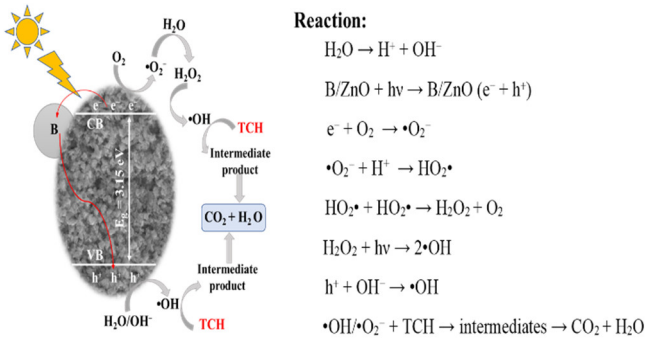

Figure 7. Photocatalytic mechanism of the 3B/ZnO material

4. CONCLUSION

In summary, the B/ZnO materials with different weight percentages of B were synthesized by a Sol-gel method. The light absorption and photocatalytic degradation of TCH of the materials have been studied and evaluated. The results showed that the optimal doping of B was 3 wt%. The 3B/ZnO material showed the best material with the band gap energy of 3.15eV, the TCH degradation efficiency of 92.28%, and the rate constant of 0.048min^{-1}. The characteristics of the ZnO and 3B/ZnO materials were analyzed, compared, and showed accurate results. The 3B/ZnO material was relatively rough and the nanoparticles were more compact. The presence of B reduced the crystallinity of 3B/ZnO material. The significant enhancement of photocatalytic performance could be explained by the recombination process between electrons and holes reduced. Moreover, the coupling of B with ZnO resulted in an enhancement of the surface area, and active sites, and attracted electrons of the 3B/ZnO material. Factors affecting the photocatalytic process of the 3B/ZnO were studied. The optimal reaction conditions of the initial TCH concentration of 20mg/L, the 3B/ZnO material content of 0.5g/L, and the solution pH 6. This is a potential catalyst material in the field of wastewater treatment, and it also helps to solve energy-related problems.

ACKNOWLEDGMENTS

Thu Huong Nguyen was funded by the Master, PhD Scholarship Programme of Vingroup Innovation Foundation (VINIF), code VINIF.2023.ThS.061

REFERENCES

[1]. T. H. Nguyen, T. A. N. Cong, and A. T. Vu, "Synthesis of Carnation-Like ZnO for Photocatalytic Degradation of Antibiotics, Including Tetracycline Hydrochloride," *Environmental Engineering Science,* 2023.

[2]. Q. Li, et al., "Enhancement of Visible-Light Photocatalytic Degradation of Tetracycline by Co-Doped TiO_2 Templated by Waste Tobacco Stem Silk," *Molecules,* 28, 1, p. 386, 2023.

[3]. D. J. Larsson, "Antibiotics in the environment," *Upsala journal of medical sciences,* 119, 2, 108-112, 2014.

[4]. C. X. Low, et al., "Unveiling the impact of antibiotics and alternative methods for animal husbandry: A review," *Antibiotics,* 10, 5, 578, 2021.

[5]. A. Kumar, A. Patyal, and A. Panda, "Sub-therapeutic use of antibiotics in animal feed and their potential impact on environmental and human health: a comprehensive review," *J. Anim. Feed Sci. Technol,* 6, 25, 2018.

[6]. N. Key, and W. D. McBride, "Sub-therapeutic antibiotics and the efficiency of US hog farms," *American Journal of Agricultural Economics,* 96, 3, 831-850, 2014.

[7]. P. M. Manage, "Heavy use of antibiotics in aquaculture; emerging human and animal health problems - a review," *Sri Lanka J. Aquat. Sci.* 23(1): 13-27, 2018.

[8]. M. Rasul, and B. Majumdar, "Abuse of antibiotics in aquaculture and it's effects on human, aquatic animal and environment," *The Saudi Journal of Life Sciences,* 2, 3, 81-88, 2017.

[9]. F. C. Cabello, "Heavy use of prophylactic antibiotics in aquaculture: a growing problem for human and animal health and for the environment," *Environmental microbiology,* 8, 7, 1137-1144, 2006.

[10]. F. C. Cabello, "Antibiotics and aquaculture in Chile: implications for human and animal health," *Revista medica de Chile,* 132, 8, 1001-1006, 2004.

[11]. B. Bojarski, B. Kot, and M. Witeska, "Antibacterials in aquatic environment and their toxicity to fish," *Pharmaceuticals,* 13, 8, 189, 2020.

[12]. M. A. Dawood, S. Koshio, and M. Á. Esteban, "Beneficial roles of feed additives as immunostimulants in aquaculture: a review," *Reviews in Aquaculture,* 10, 4, 950-974, 2018.

[13]. T. H. Nguyen, and A. T. Vu, "Preparation of B/ZnO Nanocomposite by Simple Mechanical Combustion Method for Removal of Antibiotics in Aqueous Environments," *Bulletin of Chemical Reaction Engineering & Catalysis,* 10, 2022.

[14]. T. H. Nguyen, and A. T. Vu, "Investigation of enhanced degradation of the antibiotic under visible in novel B/ZnO/TiO_2 nanocomposite and its electrical energy consumption," *Nanotechnology,* 35, 1, 015709, 2023.

[15]. C. Y. Pei, Y. G. Chen, L. Wang, W. Chen, and G. B. Huang, "Step-scheme WO_3/$CdIn_2S_4$ hybrid system with high visible light activity for tetracycline hydrochloride photodegradation," *Appl. Surf. Sci.,* 535, 147682, 2021.

[16]. M. Athari, M. Fattahi, M. Khosravi-Nikou, and A. Hajhariri, "Adsorption of different anionic and cationic dyes by hybrid nanocomposites of carbon nanotube and graphene materials over Ui0-66," *Scientific Reports,* 12, 1, 20415, 2022.

[17]. T. A. T. Pham, et al., "Facile preparation of ZnO nanoparticles and Ag/ZnO nanocomposite and their photocatalytic activities under visible light," *J. Anal. Methods Chem.,* 2020, 1-14, 2020.

[18]. L. Liu, et al., "Synergistic effect of B-TiO_2 and MIL-100 (Fe) for high-efficiency photocatalysis in methylene blue degradation," *Appl. Surf. Sci.,* 561, 149969, 2021.

[19]. T. Vu Anh, T. A. T. Pham, V. H. Mac, and T. H. Nguyen, "Facile controlling of the physical properties of zinc oxide and its application to enhanced photocatalysis," *J. Anal. Methods Chem.,* 2021, 1-12, 2021.

[20]. V. H. Mac, and A. T. Vu, "Controlling the 3D flower-like ZnO via simple precipitation method and its formation mechanism and photocatalytic application," *J. Chin. Chem. Soc.,* 69, 12, 1997-2005, 2022.

[21]. S. Ye, R. Wang, M. Z. Wu, and Y. P. Yuan, "A review on g-C_3N_4 for photocatalytic water splitting and CO_2 reduction," *Applied Surface Science,* 358, 15-27, 2015.

[22]. S. Zhang, H. S. Chen, K. Matras-Postolek, and P. Yang, "ZnO nanoflowers with single crystal structure towards enhanced gas sensing and photocatalysis," *Physical chemistry chemical physics : PCCP*, 17, 45, 30300-30306, 2015.

[23]. M. T. Le, H. L. Nguyen, A. T. Vu, V. C. Nguyen, and J. C. Wu, "Synthesis of TiO_2 on different substrates by chemical vapor deposition for photocatalytic reduction of Cr (VI) in water," *Journal of the Chinese Chemical Society,* 66, 12, 1713-1720, 2019.

[24]. T. A. N. Thi, and A. T. Vu, "Nanocomposite ZnO/g-C_3N_4 for Improved Degradation of Dyes under Visible Light: Facile Preparation, Characterization, and Performance Investigations," *Bulletin of Chemical Reaction Engineering & Catalysis,* 17, 2, 403-419, 2022.

[25]. Y. F. Cheng, et al., "Two hybrid Au-ZnO aggregates with different hierarchical structures: A comparable study in photocatalysis," *Journal of Colloid and Interface Science,* 509, 58-67, 2018.

[26]. X. Zhu, X. Liang, P. Wang, Y. Dai, and B. Huang, "Porous Ag-ZnO microspheres as efficient photocatalyst for methane and ethylene oxidation: Insight into the role of Ag particles," *Applied Surface Science,* 456, 493-500, 2018.

[27]. A. Z. Ahmed, M. M. Islam, M. M. u. Islam, S. M. Masum, R. Islam, and M. A. I. Molla, "Fabrication and characterization of B/Sn-doped ZnO nanoparticles via mechanochemical method for photocatalytic degradation of rhodamine B," *Inorganic and Nano-Metal Chemistry,* 51, 10, 1369-1378, 2020.

[28]. R. E. Núñez-Salas, J. Rodriguez-Chueca, A. Hernández-Ramírez, E. Rodríguez, and M. de Lourdes Maya-Treviño, "Evaluation of B-ZnO on photocatalytic inactivation of Escherichia coli and Enterococcus sp," *Journal of Environmental Chemical Engineering,* 9, 1, 104940, 2021.

[29]. A. T. Vu, T. H. Nguyen, and T. H. Nguyen, "Preparation of carnation-like Ag-ZnO composites for enhanced photocatalysis under visible light," *Nanotechnology,* 34, 27, p. 275602, 2023.

THÔNG TIN TÁC GIẢ

Nguyễn Thu Hương[1], Vũ Anh Tuấn[1], Nguyễn Minh Việt[2]

[1]Trường Hóa và Khoa học sự sống, Đại học Bách khoa Hà Nội

[2]Khoa Công nghệ Hoá, Đại học Công nghiệp Hà Nội